The doublesex-related Dmrta2 safeguards neural progenitor maintenance involving transcriptional regulation of Hes1

Fraser I. Young[a], Marc Keruzore[b,1], Xinsheng Nan[c,1], Nicole Gennet[a], Eric J. Bellefroid[b,2], and Meng Li[a,c,2]

[a]Neuroscience and Mental Health Research Institute, School of Medicine, Cardiff University, Cardiff CF24 4HQ, United Kingdom; [b]Institute of Neuroscience, Université Libre de Bruxelles, B-6041 Gosselies, Belgium; and [c]School of Bioscience, Cardiff University, Cardiff CF24 4HQ, United Kingdom

Edited by Anders Bjorklund, Lund University, Lund, Sweden, and approved May 16, 2017 (received for review March 29, 2017)

The mechanisms that determine whether a neural progenitor cell (NPC) reenters the cell cycle or exits and differentiates are pivotal for generating cells in the correct numbers and diverse types, and thus dictate proper brain development. Combining gain-of-function and loss-of-function approaches in an embryonic stem cell-derived cortical differentiation model, we report that doublesex- and mab-3–related transcription factor a2 (Dmrta2, also known as Dmrt5) plays an important role in maintaining NPCs in the cell cycle. Temporally controlled expression of transgenic *Dmrta2* in NPCs suppresses differentiation without affecting their neurogenic competence. In contrast, *Dmrta2* knockout accelerates the cell cycle exit and differentiation into postmitotic neurons of NPCs derived from embryonic stem cells and in Emx1-cre conditional mutant mice. Dmrta2 function is linked to the regulation of *Hes1* and other proneural genes, as demonstrated by genome-wide RNA-seq and direct binding of Dmrta2 to the *Hes1* genomic locus. Moreover, transient *Hes1* expression rescues precocious neurogenesis in *Dmrta2* knockout NPCs. Our study thus establishes a link between Dmrta2 modulation of *Hes1* expression and the maintenance of NPCs during cortical development.

Dmrta2 | Hes1 | cell cycle | transcription factor | neurogenesis

Balancing neural progenitor cell (NPC) self-renewal and neuronal differentiation is essential for generating cells in correct numbers and diverse types during brain development (1, 2). As such, cortical neurogenesis is tightly regulated by a complex array of transcription factors that work in concert to coordinate NPC maintenance and differentiation. Proneural transcription factors, such as neurogenin (Neurog) and NeuroD, act as the primary initiators of differentiation through their direct regulation of target genes associated with cytoskeletal reorganization, migration, and other critical differentiation processes (3, 4). Proneural transcription factors are themselves subject to transcriptional regulation by other cortical transcription factors, such as Pax6 and Hes1. Pax6 acts upstream to promote neuronal differentiation through its direct activation of proneural genes (5). On the other hand, the basic helix–loop–helix transcription factor Hes1 promotes NPC proliferation and self-renewal through its repressive actions on proneural gene expression, thereby restricting spontaneous differentiation (6).

Significant disruptions to this delicate regulatory network can result in severe developmental defects due to altered neuronal production (1, 2). One such disorder is microlissencephaly, a rare genetic-linked group of neurodevelopmental malformations characterized by the absence of sulci and gyri of the cerebral cortex and an accompanying reduction in cortical size and volume. Recently, a loss-of-function mutation in the doublesex- and mab-3–related transcription factor a2 (*DMRTA2*, also known as *DMRT5*) gene has been reported in a case of microlissencephaly, implicating *DMRTA2* as a critical regulator of cortical NPC dynamics (7).

Dmrta2 belongs to the highly conserved family of *Dmrt* transcription factors, whose roles in the developing reproductive system have been extensively characterized (8). Another site of expression and function of *Dmrta2* has been found in the embryonic brain, however (9, 10). *Dmrta2* loss of function in zebrafish leads to significant reductions in cortical size, coupled with reduced neuronal numbers (10, 11). Likewise, a smaller neocortex, particularly the dorsomedial neocortex, has been observed in mice carrying null deletions of *Dmrta2* (12–14). Together with the association of *DMRTA2* mutation and microlissencephaly in humans, these findings implicate *Dmrta2* as an important regulator for cortical neurogenesis.

Dmrta2-null mice also exhibit agenesis of the embryonic cortical hem, however. The cortical hem is the embryonic organizer for the hippocampus and a major regulator of cortical patterning outside the hippocampus. It provides a source of Wingless-related (WNT) and bone morphogenetic protein (BMP) signaling in the dorsomedial telencephalon to control proper cortical regionalization and NPC expansion in a paracrine fashion (15, 16). Thus, the severe patterning and arealization defects in *Dmrta2*-null model organisms prohibit a clear dissection of a direct role of *Dmrta2* in NPC behavior from the secondary effect of an overall reduction in extrinsic hem-derived signals. More recently, conditional *Dmrta2* mutant mice (*Dmrta2*$^{fl/fl}$;*Emx1-cre*), which delete *Dmrta2* in cortical progenitors after cortical hem formation, also have been found to have reduced cortical hemisphere size,

Significance

Maintaining an intricate balance between continued progenitor proliferation and cell cycle exit/differentiation is pivotal for proper brain development. Disruption of this delicate process can lead to brain malformations, such as microlissencephaly. In this paper, we identify Dmrta2 (doublesex- and mab-3–related transcription factor a2, also known as Dmrt5) as an important transcription factor that helps regulate the fine tuning between cell cycle progression and neuronal differentiation. Mechanistically, this function of Dmrta2 involves direct transcriptional regulation of a known repressor of neurogenesis Hes1. Our findings thus add Dmrta2 to the complex regulatory machinery controlling cortical NPC maintenance, and provide an explanation for the microlissencephaly caused by Dmrta2 deficiency in model organisms and humans.

Author contributions: F.I.Y., M.K., X.N., E.J.B., and M.L. designed research; F.I.Y., M.K., X.N., and N.G. performed research; F.I.Y., M.K., X.N., E.J.B., and M.L. analyzed data; and F.I.Y. and M.L. wrote the paper.

The authors declare no conflict of interest.

This article is a PNAS Direct Submission.

Freely available online through the PNAS open access option.

Data deposition: The data reported in this paper have been deposited in the Gene Expression Omnibus (GEO) database, https://www.ncbi.nlm.nih.gov/geo (accession no. GSE90827).

[1]M.K. and X.N. contributed equally to this work.

[2]To whom correspondence may be addressed. Email: LiM26@cardiff.ac.uk or ebellefr@ulb.ac.be.

This article contains supporting information online at www.pnas.org/lookup/suppl/doi:10.1073/pnas.1705186114/-/DCSupplemental.

suggesting a direct role of Dmrta2 in the control of NPC behavior that remains to be defined (14).

Embryonic stem cells (ESCs) are capable of giving rise to all somatic cell types with easy access during in vitro differentiation. Mouse and human ESCs can efficiently generate cortical NPCs in culture without any added morphogens and subsequently differentiate into layer-specific neurons in a temporally regulated fashion, recapitulating major steps of normal cortical development (17–19). In this study, we analyzed the behavior of mouse ESC-derived cortical progenitors either lacking *Dmrta2* or conditionally expressing transgenic *Dmrta2* (9). We report that enforced expression of *Dmrta2* in cortical NPCs suppresses neuronal differentiation without affecting neurogenic competence, whereas in its absence cortical NPCs undergo precocious cell cycle exit and neuronal differentiation in vitro and in vivo. We provide evidence that Dmrta2 maintains NPC status via transcriptional regulation of *Hes1*. Thus, this study identifies an additional layer of genetic control by *Dmrta2* in the fine-tuning of cortical NPC proliferation and terminal differentiation.

Results

Expression of *Dmrta2* by ESC-Derived Cortical NPCs. To achieve efficient induction of cortical fate from mouse ESCs, we incorporated in our protocol several measures previously shown to promote a dorsal telencephalic fate (Fig. 1*A*) (17). These included dual SMAD inhibition with SB431542 and LDN193189 to accelerate neural induction (20); the addition of a Wnt inhibitor, XAV, to suppress caudalization (21, 22); and the addition of cyclopamine to antagonize ventralization of NPCs by endogenous sonic hedgehog (SHH) signaling (18). (Cultures generated by this paradigm are referred to hereinafter as cortical cultures.) As negative controls for cortical identity, we induced ESCs in parallel toward a ventral telencephalic fate with SHH, a caudal fate with retinoic acid, and a ventral mesencephalic (dopaminergic) fate using a combination treatment with ERK inhibitor and SHH (Fig. S1*A*) (23).

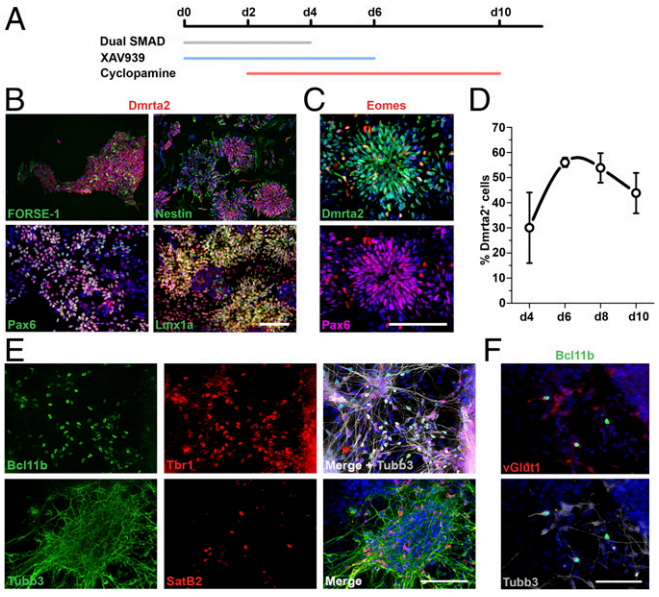

Fig. 1. *Dmrta2* expression in ESC-derived cortical NPCs. (*A*) Schematic representation of the ESC cortical differentiation protocol. (*B*) Dmrta2 immunostaining on day 6 of differentiation showing colabeling with other cortical markers. (*C*) Colocalized immunostaining of Dmrta2 and Pax6 in neural rosettes on day 8 of differentiation, with Eomes$^+$ basal progenitor extending distally. (*D*) Quantification of the proportion of Dmrta2$^+$ cells between days 4 and 10 of differentiation. Data are presented as mean ± SEM of three independent experiments. (*E*) Immunocytochemistry for deep [Bcl11b (Ctip2) and Tbr1] and superficial (Satb2) layer cortical neuronal markers at day 15. (*F*) High-magnification images of vGlut1 and Bcl11b staining in dorsal telencephalic neurons. (Scale bars: 100 μm.)

The generation of cortical NPCs was verified by immunostaining at day 6 to day 8 for cortical-specific or cortical-enriched markers Pax6, Lmx1a, Eomes (Tbr2), Otx2, Coup-TF1, and FORSE-1 (also known as LeX) along with Nestin as a pan-NPC marker (Fig. 1 *B* and *C* and Fig. S1 *B* and *D*). The vast majority of cells in the cortical cultures stained positive for Pax6, FORSE-1, Otx2, Lmx1a, Coup-TF1, and Nestin, whereas a proportion of cells also expressed Eomes. The transcription factor Nkx2.1 is specifically expressed by medial ganglionic eminence progenitors. Although abundant Nkx2.1$^+$ cells were detected in SHH-treated ventral telencephalic cultures, negligible numbers of Nkx2.1$^+$ cells were found in cortical cultures (Fig. S1*B*). Foxa2 is a marker for the ventral midbrain and spinal cord. Few Foxa2$^+$ cells were observed in the cortical cultures, whereas they constituted the major population in dopaminergic differentiated cultures (Fig. S1*C*).

Double immunocytochemistry showed that Dmrta2$^+$ cells were confined to Nestin$^+$ and FORSE-1$^+$ NPCs in cortical cultures, representing 30–54% of the total cell population between day 4 and day 10 (Fig. 1 *B* and *D*). During development, *Dmrta2* expression is restricted to the dorsal telencephalon, where it is coexpressed with *Pax6* but in an opposite gradient (12, 13, 24). Consistent with its expression in vivo, we found that Dmrta2 and Pax6 staining largely overlapped in ESC-derived NPCs localized in neural rosettes, from which Eomes$^+$ basal progenitor cells could be seen extending distally (Fig. 1*C*). In contrast, no Dmrta2$^+$ cells were found in SHH- or retinoic acid-treated NPC cultures (Fig. S1 *B* and *D*).

Dmrta2$^+$ cells were no longer detectable by day 15 of differentiation. At this stage, the presence of postmitotic cortical neurons was confirmed by immunostaining for cortical layer-specific neuronal markers Tbr1 (layer VI), Bcl11b (Ctip2; layers V and VI), and Satb2 (layer II/III) and a pan-glutamatergic neuronal marker, vGlut1 (Fig. 1 *E* and *F* and Fig. S1*E*). Very few GABAergic neurons, identified by GAD65/67 immunostaining, were observed in the cortical cultures (Fig. S1*E*). Moreover, we did not observe TH$^+$/Nurr1$^+$ dopaminergic neurons or Isl1$^+$/Olig2$^+$ spinal motor neurons, confirming an enrichment of cortical neurons in our cultures (Fig. S1 *F* and *G*). Taken together, our data demonstrate the ability to reproduce in vitro Dmrta2$^+$ dorsal telencephalic NPCs and their neuronal progeny.

Enforced Expression of Dmrta2 Suppresses NPC Neuronal Differentiation. To investigate a role for Dmrta2 in telencephalic NPC behavior, we first examined the effect of Dmrta2 gain of function in neuronal differentiation of ESC-derived NPCs using a tetracycline-inducible *Dmrta2* transgenic mESC model (*Dmrta2*-ESCs) reported previously (9). These cells harbor the reverse tetracycline-controlled transactivator (rtTA) and produce significant levels of Dmrta2 protein in response to the addition of doxycycline to the culture medium. The *Dmrta2* transgene was induced at the peak of NPC production for 7 d starting at day 5, and the expression of several neurogenic genes was examined by quantitative PCR (qPCR) (Fig. 2 *A* and *B*). In the control condition, without doxycycline, the level of proneural gene transcripts (*Neurog2*, *Neurod1*, and *Neurod4*) increased gradually from day 6, along with the immature neuronal marker gene *Tubb3* (β3-tubulin); however, lower levels of all these transcripts were detected in parallel sister cultures treated with doxycycline at all time points analyzed. In contrast, the transcript levels of *Hes1*, a repressor of cortical neurogenesis, was robustly up-regulated (Fig. 2*B*). These gene expression changes were concurrent with the induced transgenic *Dmrta2* from day 6, which remained at a higher level than in control cultures throughout.

Consistent with the qPCR observations, cells exposed to doxycycline for 5 d maintained a largely NPC morphology, whereas the sister control cells progressed to terminal differentiation into neurons (Fig. 2*C*). Immunostaining confirmed a marked reduction

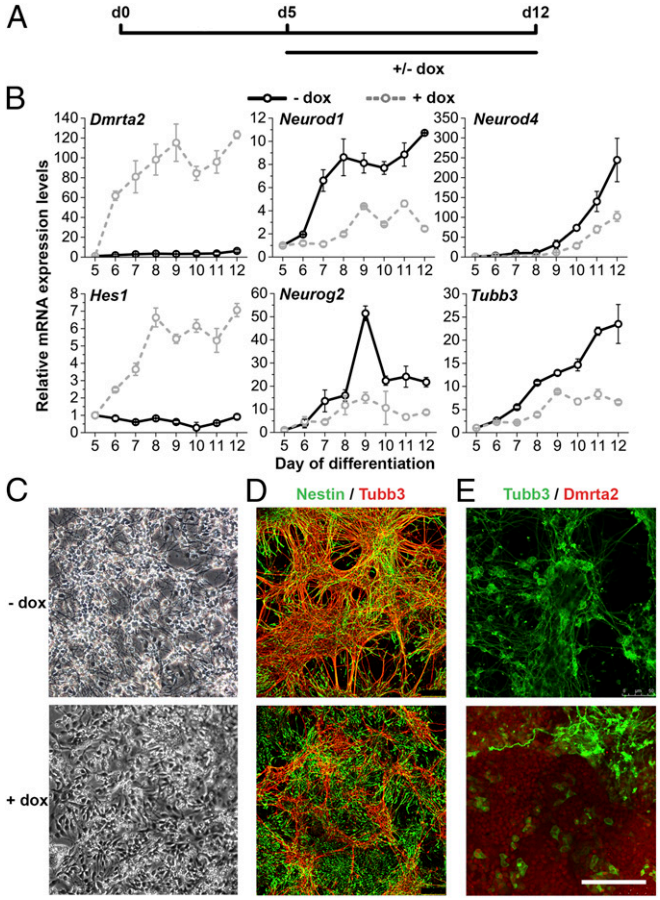

Fig. 2. Enforced expression of Dmrta2 in NPCs suppresses neuronal differentiation. (*A*) Experimental scheme. Monolayer cultures of *Dmrta2*-ESCs were exposed to doxycycline or vehicle control from day 5 to day 12. Cultures were harvested every day from day 6 to day 12, and samples were processed for qPCR. (*B*) qPCR analysis of the genes indicated from day 6 to day 12. Levels of mRNA expression were normalized to day 5. Error bars indicate mean ± SEM of three biological replicates. (*C*) Phase-contrast view of day 10 cultures treated with doxycycline (*Bottom*) or vehicle (*Top*) from day 5. (*D*) Sister cultures as in *C* double-stained with antibodies against Nestin (green) and Tubb3 (red). (*E*) Day 10 cultures as in *C* double-stained for Tubb3 (green) and Dmrta2 (red). (Scale bars: 100 μm.)

of Tubb3$^+$ cells in doxycycline-treated cultures compared with controls. In contrast, doxycycline-treated cultures contained more Nestin$^+$ NPCs (Fig. 2*D*). Moreover, double immunocytochemistry for Dmrta2 and Tubb3 revealed mutually exclusive staining in doxycycline-treated cultures, providing direct evidence that a high level of Dmrta2 suppresses the neuronal differentiation of NPCs (Fig. 2*E*).

Interestingly, on removal of doxycycline after 4 d of treatment, the NPCs readily gave rise to Tubb3$^+$ neurons (Fig. S2). This finding suggests that a high level of Dmrta2 favors NPC maintenance over neuronal differentiation without affecting their neurogenic competence.

Loss of Dmrta2 Accelerates Neuronal Differentiation of Cortical NPCs. To gain further insight into the physiological function of Dmrta2 in neurogenesis and the cellular mechanisms that might underpin the microcephaly caused by Dmrta2 loss-of-function mutation, we generated lines of mESCs with homozygous deletion of *Dmrta2* (*Dmrta2*$^{-/-}$) by gene targeting and directed these cells toward a cortical fate (Fig. 3 and Fig. S3). We closely monitored neural induction and neuronal differentiation in *Dmrta2*$^{-/-}$ and isogenic control (*Dmrta2*$^{flox/flox}$) cultures by immunocytochemistry and qPCR (Fig. 3 *A* and *B*). Rapid neuroepithelial fate conversion was observed in both genotypes, as demonstrated by the generation of a similar proportion of Nestin$^+$ NPCs at days 4 and 6 (Fig. 3*A*). However, following the onset of *Dmrta2* expression at day 4, we observed marked differences in the temporal expression profile of the intermediate progenitor marker gene *Eomes*, neuronal marker *Map2*, and proneural transcription factors *Neurog2* and *Neurod1* (Fig. 3*B*). *Map2* and *Eomes* levels were increased in the *Dmrta2*$^{-/-}$ cultures, whereas both *Neurog2* and *Neurod1* RNA reached their highest levels sooner in *Dmrta2*$^{-/-}$ cells compared with control cells, suggesting early initiation of a neurogenesis program. Consistent with this observation, we detected an increase in the production of Tubb3$^+$ neurons in *Dmrta2*$^{-/-}$ cultures by immunostaining at days 4, 6, and 8 compared with the isogenic control cultures (Fig. 3*C*). Similarly, *Dmrta2*$^{-/-}$ cultures also contained significantly more NeuN$^+$ cells (mature neurons) at days 10–14 (Fig. 3*D*).

In the reduced cortex of *Dmrta2*$^{-/-}$ embryos, a transient increase in neuronal production also has been observed during early corticogenesis. This excess neuronal production during early neurogenesis may be a secondary consequence of the reduction of Wnt cortical hem signals or a direct consequence of the loss of *Dmrta2* in cortical progenitors (12). To test this latter possibility, we used immunostaining to assay the amount of Tubb3$^+$ and Eomes$^+$ cells in the cortical plate of E11 conditional *Dmrta2* mutant mice (*Dmrta2*$^{fl/fl}$;*Emx1-cre*), in which the Wnt signaling pathway appears to be unaffected (14). We found increased numbers of Tubb3$^+$ and

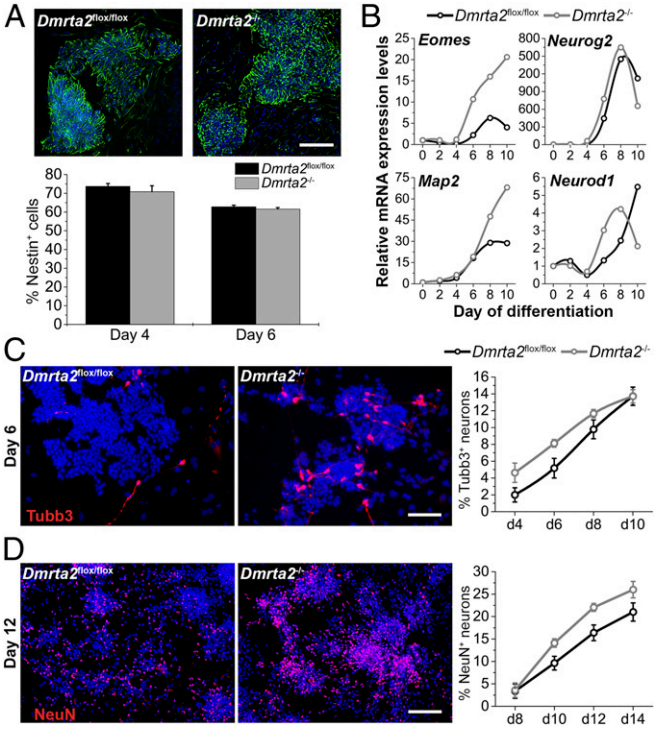

Fig. 3. Loss of *Dmrta2* in cortical NPCs accelerate neurogenesis in vitro. (*A*) Day 4 and day 6 cultures were immunostained for Nestin, revealing comparable generation of NPCs in the control and *Dmrta2*$^{-/-}$ cultures. (*B*) qPCR analysis of neuronal differentiation markers. Data are representative of three independent differentiation experiments. (*C*) Immunostaining and quantification of cells expressing an immature neuronal marker, Tubb3. Two-way ANOVA identified a significant increase in the overall production of Tubb3$^+$ neurons by Dmrta2$^{-/-}$ NPCs ($F_{1,16} = 8.005$; $P = 0.012$). (*D*) Immunostaining and quantification of cells expressing mature neuronal marker NeuN. Two-way ANOVA revealed a significant increase in the overall maturation of neurons derived from Dmrta2$^{-/-}$ NPCs ($F_{1,16} = 11.991$; $P = 0.003$). (Scale bars: 100 μm.)

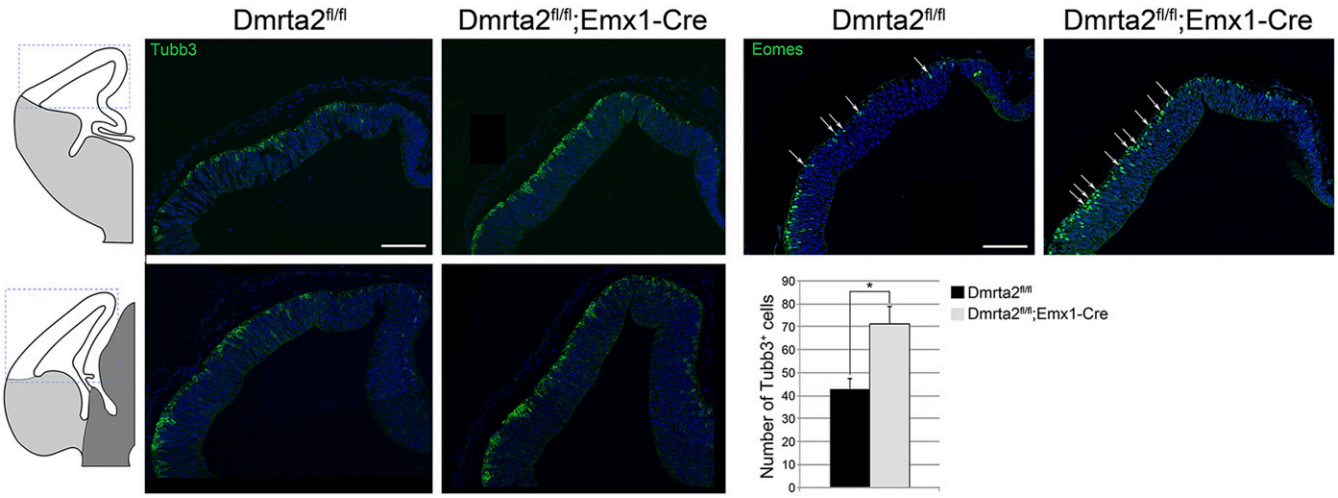

Fig. 4. Loss of *Dmrta2* in cortical NPCs accelerate neurogenesis in vivo. Immunostaining of Tubb3 (*Left*) and Eomes (*Right*) on coronal brain sections of E11 embryos. Note the increase of Tubb3$^+$ and Tbr2$^+$ cells (arrows in *Right*) in the *Dmrta2$^{fl/fl}$;Emx1-Cre* mutants compared with controls. The graph is a representation of the number of Tubb3$^+$ cells in *Dmrta2$^{fl/fl}$;Emx1-Cre* and control embryos. Data are mean ± SEM of three independent experiments; *P < 0.05, two-tailed Student's t test. (Scale bars: 100 μm.)

Eomes$^+$ cells in the conditional *Dmrta2* mutant mice relative to controls (Fig. 4). Thus, premature neuronal differentiation is also a feature in vivo of conditional *Dmrta2* mutant mice, corroborating our in vitro observations and suggesting a direct role for Dmrta2 in cortical NPC neurogenesis.

Altered Dmrta2 Levels Lead to Cell Cycle Dysregulation in Cortical NPCs. Disruptions of cortical NPC proliferation and cell cycle progression have been implicated as underlying mechanisms for microlissencephaly (25). To determine whether Dmrta2 plays a role in cell cycle regulation, we performed a flow cytometry-based cell cycle analysis to reveal the distribution of Nestin$^+$ NPCs in three major phases of the cell cycle: G0/1, S, and G2/M (Fig. 5*A*). We found significantly more *Dmrta2$^{-/-}$* cortical NPCs than control cells in the G0/1 phase (P < 0.01) at day 6 of differentiation (Fig. 5*B*). Accordingly, the number of cells in the S phase was reduced (P < 0.05) in day 6 *Dmrta2$^{-/-}$* NPCs compared with controls, although no differences were seen on days 8 and 10.

To gain further insight into Dmrta2-regulated cell cycle progression, we carried out EdU incorporation assays at days 6, 8, and 10 of differentiation. These assays revealed a reduced number of EdU-labeled cells in *Dmrta2$^{-/-}$* cultures compared with control cultures at all three time points, providing independent evidence of altered S phase in *Dmrta2$^{-/-}$* NPCs (Fig. 5*C*). Moreover, an immunocytochemical analysis showed that the numbers of cells expressing Cdkn1b (p27kip1) and Cdkn1c (p57Kip2) were increased in *Dmrta2$^{-/-}$* cultures compared with controls (Fig. 5*C*). Cdkn1b and Cdkn1c are cell cycle regulators with a major function in halting or slowing the G1-S phase transition, and thus their up-regulation is closely associated with cell cycle exit and neuronal differentiation. In contrast, we observed a reduction at the transcript level of these two cell cycle regulators and an increase in the proportion of Ki67$^+$ cells when NPCs were forced to express Dmrta2 (Fig. S4). Taken together, these findings identify an unexpected role for Dmrta2 in NPC cell cycle regulation, and suggest that the disrupted regulation of cell cycle progression in *Dmrta2$^{-/-}$* NPCs may be a significant contributor to the precocious neurogenesis described above.

Genome-Wide Transcriptome Profiling Supports a Role for Dmrta2 in NPC Neurogenesis. To gain insight into the molecular mechanisms underlying the altered neurogenesis in *Dmrta2*-deficient NPCs, we carried out a transcriptome analysis by RNA sequencing (RNA-seq) using day 8 cultures, a timepoint associated with the highest number of Dmrta2$^+$ cells and when both neurogenic and proliferative defects were apparent. Analysis of this RNA-seq dataset identified 7,343 differentially expressed transcripts at a significance level of P < 0.05 (Fig. 6*A*, Fig. S5, and Dataset S1). Among the *Dmrta2*-regulated genes were transcription factors involved in cortical development and patterning, including *Foxg1*, *Pax6*, *Emx1*, *Emx2*, *Nr2f1 (Coup-TF1)*, and *Sp8* (Fig. 6 *B* and *C*). Similarly, *Lmx1a* and *Msx1*, genes associated with development of the cortical hem, were significantly down-regulated in *Dmrta2$^{-/-}$* cultures. Interestingly, *Dmrta2* itself was identified as one of the most significantly up-regulated transcripts on loss of *Dmrta2* (Fig. 6*B* and Fig. S5*C*). The closely related *Dmrt* family member *Dmrta1* was also up-regulated in *Dmrta2$^{-/-}$* NPCs, whereas no significant change was found for *Dmrt3*. In the reduced cortex of *Dmrta2* conditional mutants, *Dmrta2* and *Dmrta1* also have been found to be up-regulated (14). Taken together, these observations further support a negative autoregulatory function for *Dmrta2*, as well as regulatory interactions with other *Dmrt* family members.

We are particularly interested in genes and gene sets that have a functional role in NPC proliferation and/or neuronal differentiation. Our data reveal a significant down-regulation of *Hes1* (Fig. 6*C*). Down-regulated expression also was identified for other transcription factors known to complex with *Hes1* to repress proneural gene expression and promote NPC proliferation, including *Id1*, *Id3*, and *Tcf3* (6, 26, 27). In contrast, we found an up-regulation in the expression of *Hes1* target proneural genes *Neurog1*, *Neurog2*, and *Ascl1*, together with their downstream target genes *Neurod1*, *Neurod4*, and *Nhlh1 (*3, 4*)*. Furthermore, genes known to perform opposing actions to *Hes1* by promoting the expression of proneural genes, including *Pax6* and *Btg2*, were up-regulated (5, 28). Other up-regulated transcription factors with proneuronal functions included *Insm1*, *Myt1l*, and *Brn2* (29, 30). Consistent with these findings, molecular markers for intermediate progenitor (*Eomes*), immature (*Dcx*), and mature (*Mapt*, *Nefh*, and *Rbfox3*) neurons also were up-regulated in *Dmrta2$^{-/-}$* cells (Fig. 6*D*).

To provide a broader overview of the cellular functions of *Dmrta2*-regulated genes/gene sets, we performed a Gene Ontology (GO) functional enrichment analysis using gene lists meeting the stringent criteria of P < 0.01 and an absolute fold change value >2. This analysis revealed that the 650 up-regulated genes meeting these criteria are enriched in transcripts associated with biological processes including neuronal differentiation,

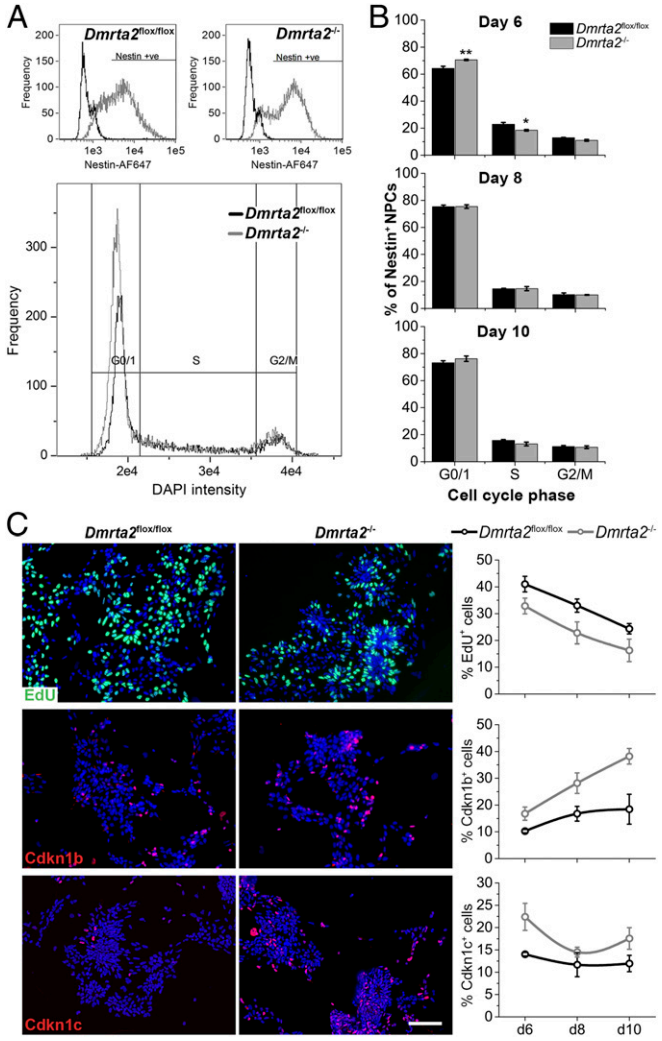

Fig. 5. Disruption of cell cycle progression in *Dmrta2*$^{-/-}$ NPCs. (*A*) Cell cycle analysis of *Dmrta2*$^{flox/flox}$ and *Dmrta2*$^{-/-}$ NPCs by flow cytometry. NPCs were first immunostained with antibodies against Nestin (*Top*), and DNA content was measured by DAPI labeling (*Bottom*). (*B*) Quantification of cell distribution in G0/1, S and G2/M phases of the cell cycle. Data are presented as mean ± SEM of three independent experiments. **P* < 0.05, ***P* < 0.01, two-way ANOVA ($F_{1,12}$ = 7.109; *P* = 0.021), followed by Sidak's post hoc test. (*C*) Quantification of EdU uptake, and the number of cells expressing cdkn1b (p57kip1) and cdkn1c (p57kip2). Two-way ANOVA identified overall reduced proliferation in *Dmrta2*$^{-/-}$ NPCs, as indicated by EdU uptake ($F_{1,12}$ = 11.336; *P* = 0.006), and an increase in the proportion of cells staining positive for Cdkn1b ($F_{1,12}$ = 20.804; *P* < 0.001) and Cdk1nc ($F_{1,12}$ = 10.477; *P* = 0.007). Data are presented as mean ± SEM of three independent experiments. (Scale bar: 100 μm.)

neurogenesis, and nervous system development in general (Fig. S5*A*). Similarly, enrichments for genes linked to the regulation of cell proliferation, organ morphogenesis, and locomotion were identified in 936 transcripts down-regulated in *Dmrta2*$^{-/-}$ cortical NPCs (Fig. S5*B*). Overall, our global gene expression analysis provides strong independent support for the role of Dmrta2 in balancing NPC proliferation and neurogenesis.

Dmrta2-Controlled Neuronal Differentiation Involves Direct Regulation of *Hes1*. The significant down-regulation of *Hes1* revealed by the RNA-seq analysis, along with its robust induction in response to *Dmrta2* transgene expression in NPCs, suggest that Dmrta2 may maintain cortical NPC status via regulation of *Hes1* transcription. To determine whether this is mediated by direct binding of Dmrta2, we performed chromatin immunoprecipitation (ChIP) on day 8 *Dmrta2*$^{flox/flox}$ NPCs, with *Dmrta2*$^{-/-}$ NPCs serving as a negative control. Based on the published consensus binding sequence for Dmrta2, we identified three potential binding sites (Bs1–3) at the *Hes1* locus (Fig. 7*A*) (31). Dmrta2-immunoprecipitation of DNA fragments at each of these sites was quantified relative to a non-bound control region (NBCR) by qPCR (Fig. 7*B*). An enrichment in Dmrta2-bound fragments was identified at binding sites Bs1 and Bs2 (*P* < 0.05), but not at Bs3, in *Dmrta2*$^{flox/flox}$ cells. In contrast, no enrichment was detected at any of the three potential binding sites in *Dmrta2*$^{-/-}$ control cells. Thus, Dmrta2 binds to the *Hes1* gene in NPCs.

To provide evidence for Dmrta2 regulatory activity at Bs1 and Bs2, we performed reporter assays using a *Hes1* promoter-driven luciferase vector (32). A twofold higher basal *Hes1* promoter activity level was recorded in the isogenic *Dmrta2*$^{flox/flox}$ cultures relative to the *Dmrta2*$^{-/-}$ NPCs on day 8 of differentiation (*P* < 0.001) (Fig. 7*C*). An A > C point mutation at position −3 of the binding motif has been shown to significantly impair the ability of Dmrta2 to bind to its target sequence (31); thus, we introduced A > C point mutations at Bs1 and Bs2 via site-directed mutagenesis to yield two mutated reporter constructs, p*Hes1*-luc-Bs1g.2007A > C and p*Hes1*-luc-Bs2g.2365A > C, respectively. The mutation at Bs1, but not that at Bs2, resulted in a significant reduction of elevated *Hes1* promoter activity level in *Dmrta2*$^{flox/flox}$ NPCs relative to the parental luciferase construct (*P* < 0.01), suggesting reduced binding of Dmrta2 to the mutated Bs1 (Fig. 7*C*). Taken together, these data strongly support the ability of Dmrta2 to bind to and regulate the transcriptional activity at Bs1 on the *Hes1* genomic locus.

We next sought to determine the extent to which reduced *Hes1* expression in *Dmrta2*$^{-/-}$ NPCs may contribute to their altered neurogenesis. To this end, we transfected *Dmrta2*$^{flox/flox}$ and *Dmrta2*$^{-/-}$ NPCs with a *Hes1* expression vector on day 6 of differentiation together with a GFP-coding plasmid to distinguish between *Hes1*-transfected and nontransfected cells (Fig. 7*D*). By quantifying Tubb3 staining at 48 h posttransfection, we identified significantly increased numbers of neurons in the nontransfected population of *Dmrta2*$^{-/-}$ cells relative to nontransfected isogenic controls (*P* < 0.01). As predicted based on known Hes1 function, *Hes1* transgene expression led to reduced neuronal production for each cell line. Interestingly, we found no significant differences between cell lines in the *Hes1*-transfected populations.

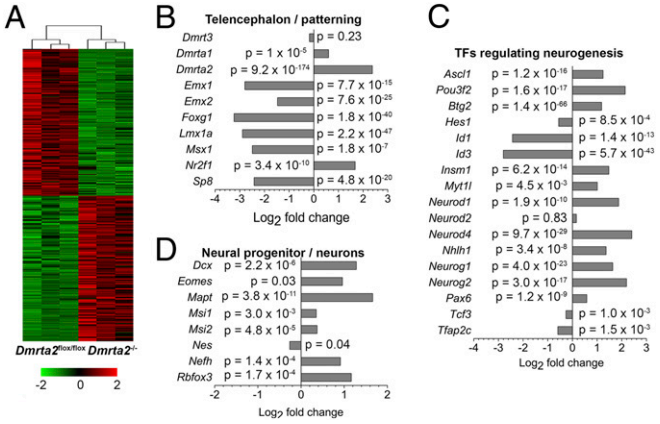

Fig. 6. Genome wide transcriptome analysis supports a role for Dmrta2 in neurogenesis. (*A*) Heatmap depicting 7343 differentially expressed mRNA transcripts (*P* < 0.05) identified by RNA-seq. (*B–D*) Examples of differentially expressed genes associated with telencephalic patterning and development (*B*), transcription factors known to regulate neuronal differentiation (*C*), and markers of different stages of neuronal maturation (*D*).

Thus, *Hes1* transgene expression leads to a rescue of the precocious neurogenesis associated with the loss of Dmrta2.

We then asked whether siRNA-mediated knockdown of *Hes1* expression could attenuate the antineurogenic effect of *Dmrta2* transgenic expression in cortical NPCs. *Dmrta2* ESCs were treated with doxycycline and *Hes1* siRNA or a control nontargeting siRNA from day 5 to day 12 of differentiation. *Hes1* knockdown resulted in a significant reduction of Nestin$^+$ NPCs ($P < 0.05$) and a concurrent increase in the proportion of Tubb3$^+$ neuronal cells (Fig. 7*E*). Thus, Hes1 knockdown partially reverses Dmrta2-mediated suppression of neuronal differentiation.

Taken together, our data identify *Hes1* as a downstream target of Dmrta2 transcriptional regulation and a mechanism through which Dmrta2 safeguards NPCs from premature differentiation.

Discussion

Dmrta2 in NPC Cell Cycle Regulation. Loss-of-function mutations in *Dmrta2* have been linked with microcephaly in zebrafish, mice, and humans (7, 10–13); however, the role and mechanism of action of Dmrta2 in the control of NPC maintenance and expansion have remained unknown until now. Recently, conditional *Dmrta2* mutant mice (*Dmrta2$^{fl/fl}$;Emx1-cre*) were created that delete *Dmrta2* in cortical progenitors after cortical hem formation without impacting Wnt signaling. The Dmrta2 cKO embryos also show reduced cortical hemisphere size, suggesting a direct role of Dmrta2 in the control of NPC behavior (14). Cells in a monolayer ESC-neural differentiation system are generally exposed to the same extracellular environment and do not form "signaling centers," unlike those found in the developing brain. Moreover, daily changes of culture medium will reduce the impact of any secreted molecules that may elicit a secondary effect. Our pathway analysis of the RNA-seq data did not reveal any significant changes in Wnt signaling; thus, the observed effect of Dmrta2 on cell cycle changes is likely cell-autonomous.

In line with the accumulation of *Dmrta2*$^{-/-}$ NPCs in the G0/G1 phase of the cell cycle, we found altered expression of various cell cycle regulatory genes, particularly those acting on the G1-to-S phase transition (*Cdkn1b*, *Cdkn1c*, and *Btg2*). Considered together, these data suggest a disruption in cell cycle progression and potential lengthening of the G1 phase in *Dmrta2*$^{-/-}$ NPCs. During normal corticogenesis, the duration of the G1 phase is linked to neuronal differentiation and is always longer in cells committed to undergoing differentiative rather than proliferative division (33, 34). Furthermore, experimental lengthening of the G1 phase pharmacologically or by the induction of *Cdkn1b* or *Cdkn1c* expression promotes neuronal differentiation and depletion of the NPC pool, resulting in microcephaly (1, 33, 35). The observed increases of *Cdkn1b* and *Cdkn1c* in *Dmrta2*$^{-/-}$ NPCs

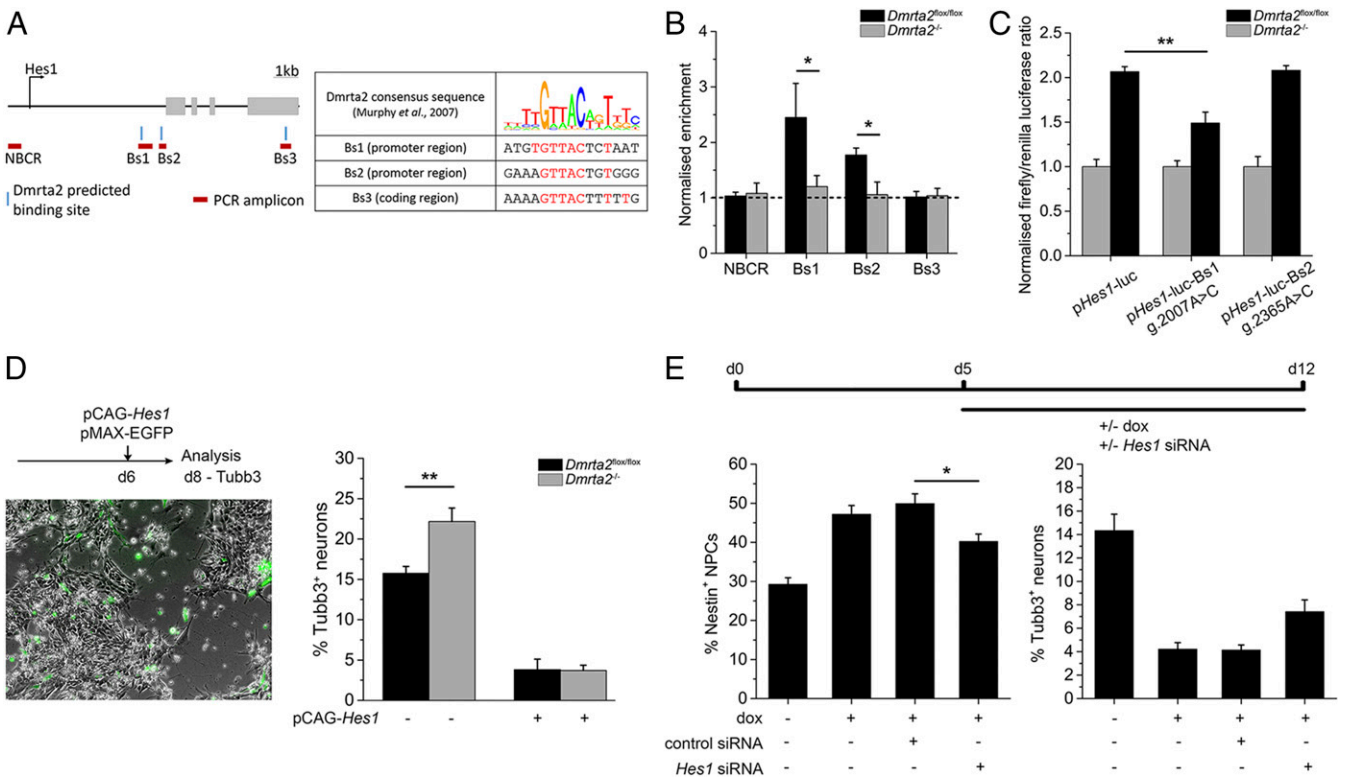

Fig. 7. *Hes1* is a direct target for Dmrta2 transcriptional regulation in NPCs. (*A*) Schematic representation of the *Hes1* genomic locus showing the relative positions of predicted Dmrta2 binding sites (Bs1–Bs3) and nonbinding control region (NCBR), and the primer pairs used to amplify each region after ChIP. (*B*) ChIP-qPCR for each of the regions depicted in *A* using chromatin prepared from *Dmrta2*$^{flox/flox}$ and *Dmrta2*$^{-/-}$ NPCs on day 8 of differentiation. Data are presented as mean ± SEM fold enrichment relative to the NBCR of three immunoprecipitations, each prepared from an independent differentiation experiment. *$P < 0.05$, one-tailed Student's *t* test. (*C*) Reporter assay performed in *Dmrta2*$^{flox/flox}$ and *Dmrta2*$^{-/-}$ NPCs on day 8 of differentiation using WT or mutant *Hes1* promoter-luciferase vectors carrying a point mutation at Bs1 or Bs2, respectively. Data are presented as mean ± SEM of three independent transfections with reporter plasmids. **$P < 0.01$, one-way ANOVA with Tukey's HSD post hoc test. (*D*) *Dmrta2*$^{flox/flox}$ and *Dmrta2*$^{-/-}$ NPCs were cotransfected with GFP and *Hes1* expression vectors on day 6 of differentiation. Cultures were immunostained for Tubb3 at 48 h later. Successfully transfected cells overexpressing *Hes1* were identified based on GFP expression. Data are presented as mean ± SEM of three transfections, each from an independent differentiation experiment. *$P < 0.05$, two-tailed Student's *t* test. (Magnification: 10×.) (*E*) Monolayer cultures of *Dmrta2*-ESCs were exposed to doxycycline with or without nontargeting control or Hes1 siRNA from day 5. The proportions of Nestin$^+$ NPCs and Tubb3$^+$ neurons were quantified at day 12. Data are presented as mean ± SEM of >20 individual fields of view. **$P < 0.05$, one-way ANOVA with Tukey's HSD post hoc test.

strongly implicate delayed cell cycle progression of *Dmrta2*$^{-/-}$ NPCs as a cellular mechanism contributing to precocious neurogenesis. Whether this is achieved through the direct regulation of cell cycle progression genes by Dmrta2 is unclear, however. Although various G1-to-S transition regulatory molecules are known to act as downstream targets for *Hes1* repression, *Cdkn2c* (p18ink4c) also has been identified as a candidate gene for direct *Dmrta2*-mediated regulation in the zebrafish testes (11, 36, 37). Our findings demonstrate that through a direct or indirect effect, Dmrta2 is intricately linked to the control of cell cycle progression, a feature conserved across species and tissues.

Along with their function in the regulation of cell cycle progression, cyclin-dependent kinase inhibitors, including *Cdkn1b*, directly influence and promote NPC differentiation by stabilizing protein levels of *Neurog2* via direct binding and the regulation of both interkinetic and radial migration (35, 38, 39). Our transcriptome analysis of *Dmrta2*$^{-/-}$ NPCs identified an enrichment of down-regulated transcripts associated with GO terms for cell adhesion (GO:0007155) and locomotion (GO:004001). Thus, it is possible that defective migration is a cellular phenotype associated with the loss of *Dmrta2* that could potentially lead to increased neuronal differentiation. Similarly, our RNA-seq data allude to a potential switch in the mode of cell division of *Dmrta2*$^{-/-}$ NPCs. The transcription factors *Emx2* and *Pax6* were found to be down-regulated and up-regulated, respectively, by *Dmrta2*$^{-/-}$ NPCs, as well as in the brains of *Dmrta2*-null mice (12). Regarding its role in telencephalic patterning, Emx2 is known to promote symmetric proliferative division of NPCs and Pax6 asymmetric differentiative division (40, 41). Thus, a switch in the mode of proliferation to neurogenic divisions may be a further cellular factor contributing to increased differentiation in the absence of Dmrta2. This idea is supported by the strong up-regulation of mRNA transcripts for *Btg2*, which is expressed exclusively in cortical NPCs committed to undergoing neurogenic, but not proliferative, division (42). Thus, although we provide evidence that *Dmrta2* safeguards NPCs from precocious neurogenesis via regulation of *Hes1*, other targets also may contribute to the fine control of neurogenesis by *Dmrta2*.

Dmrta2 Targets and Neurogenesis. To date, *Hes1* and *Cdkn2c* are the only two transcriptional targets that have been proposed for *Dmrta2*. Owing to high levels of conservation in DNA-binding motifs between Dmrt proteins, further insight may be provided by examining DNA-binding sites of related Dmrt family members in other tissues (31). Close to 1,400 direct binding sites for Dmrt1 in the mouse testis have been identified using ChIP-chip techniques (43). Many of these genes also were identified as dysregulated by our *Dmrta2*$^{-/-}$ NPC transcriptome analysis, including *Cdkn2c*, *Igf2r*, *Meis1*, *Hox* family members, and other *Dmrt* genes. Although *Dmrt1* is not expressed by cortical NPCs, our data suggest significant overlaps in the regulatory targets of different *Dmrt* proteins. This is of particular interest because of the similar expression patterns of *Dmrt*3, *Dmrta1*, and *Dmrta2* in the dorsal telencephalon, suggesting a potential for functional redundancy (13, 24). A similar but less severe phenotype as that seen in *Dmrta2* null mutants has been observed in mice with a *Dmrt3* null mutation, further supporting the idea that the two factors have overlapping functions in cortical development (12-14). In contrast, *Dmrta1*-null mice produce viable offspring with no overt anatomic defects in the brain (13, 44). This implies a hierarchical structure of importance of the *Dmrt* proteins to cortical development. Similar to our transgenic *Dmrta2* findings, forced expression of *Dmrt3* or *Dmrta1* in the rodent telencephalon is linked to the regulation of *Neurog2* expression (24). Further studies may reveal the extent of this functional overlap among Dmrt family members in the dorsal telencephalon.

The functions of the Notch target gene *Hes1* in maintaining NPC self-renewal have been well characterized (6). Notch ligands produced by newborn neurons activate notch signaling in neighboring cells, which in turn induces expression of Hes1 to repress the transcription of proneural factors and cell cycle progression regulators, thereby inhibiting neuronal differentiation (6, 36, 37). This lateral inhibition of spontaneous neuronal differentiation by neighboring cells favors NPC proliferation and self-renewal; however, *Hes1* expression is dynamically regulated by various mechanisms, including a strong negative autoregulatory function, which is in turn inhibited by interactions with Id proteins (45, 46); the activity of other transcription factors, such as Lhx2 (47); and the activation of signaling pathways by growth factors and mitogens, including Fgf2 and Notch (6, 48). Under healthy conditions, these homeostatic mechanisms help maintain a NPC pool through development by regulating the expression of *Hes1* and thus the balance between progenitor cell self-renewal and differentiation. This study has thus identified a previously unrecognized role for *Dmrta2* in the dynamic regulation of *Hes1* expression in cortical NPCs. By promoting *Hes1*, and thereby suppressing downstream proneural gene expression, *Dmrta2* contributes to the maintenance of NPC self-renewal (Fig. 8*A*). In the absence of *Dmrta2*, *Hes1* levels are reduced, leading to the up-regulation of proneural genes and increased neuronal differentiation (Fig. 8*B*).

In summary, we have identified *Dmrta2* as a modulator controlling neuronal differentiation of cortical NPCs and have provided evidence that *Dmrta2* exerts this function, at least in part, by direct transcriptional regulation of the neurogenesis inhibitor *Hes1*. Thus, this work points to another layer of control mechanisms coordinating NPC maintenance and neurogenesis, and begins to elucidate how *Dmrta2* loss-of-function mutations may lead to microcephaly.

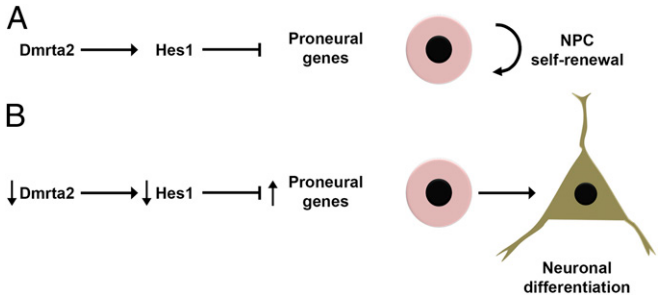

Fig. 8. Dmrta2 modulates neurogenesis through regulation of *Hes1*. Schematic model depicting the function of *Dmrta2* in the modulation of NPC maintenance and neuronal differentiation. (*A*) High *Dmrta2* expression in cortical NPCs ensures high expression of *Hes1* and low levels of proneural genes, thereby promoting NPC maintenance and cortical expansion. (*B*) On differentiation, *Dmrta2* expression declines, resulting in reduced levels of *Hes1* and increased expression of proneural genes, thereby enhancing the differentiation of NPCs into postmitotic neurons.

Materials and Methods

Cell Culture. Six mouse ESC lines were used: a *Dmrta2*$^{flox/flox}$ control line and two *Dmrta2*$^{-/-}$ lines derived from the control line (*SI Materials and Methods*), two independent doxycycline-inducible *Dmrta2*-overexpressing ESC lines, and their parental lines harboring rtTA, as reported previously (9). All ESCs were maintained under standard conditions as described previously (17). For monolayer-based cortical differentiation, ESCs were seeded at 10,000 cells/cm^2 in gelatin-coated six-well plates and cultured in N2B27 medium. The differentiation medium was supplemented with 100 nM LDN193189 (Tocris) and 10 μM SB431542 (Tocris) from day 0 to day 4, 1 μM XAV939 (Tocris) from day 0 to day 6, and 1 μM cyclopamine (Sigma-Aldrich) between days 2 and 10. On day 5 or 6 of differentiation, NPCs were dissociated using trypsin/EDTA and then replated onto a poly-D-lysine/laminin–coated surface at a density of 50,000 cells/cm^2 for neuronal differentiation and maturation.

Transient transfections were performed using Lipofectamine 3000 reagent (Thermo Fisher Scientific). The following vectors were used: p*Hes1*(2.5k)-luc (Addgene) (32), pGL4.73[hR*luc*/SV40] (Promega), pCAG-*Hes1*-IP (Lonza), and pmaxGFP (Lonza). Accell *Hes1* and nontargeting control siRNA (GE Dharmacon) were used at a concentration of 1 μM.

Mouse Lines. *Emx1-cre* and *Dmrta2*$^{fl/fl}$ mouse lines were generated and maintained as described previously (14). The experiments were performed in compliance with the relevant laws and institutional guidelines and were approved by the local ethics committee (Universite Libre de Bruxelles).

qPCR. Total RNA was extracted using TRI reagent treated with TURBO DNase (Thermo Fisher Scientific). cDNA was generated using the qScript cDNA Synthesis Kit (Thermo Fisher Scientific). qPCR was performed with MESA GREEN qPCR Master Mix (Eurogentec) with specific primers listed in Table S1, and dissociation curves were recorded to check for amplification specificity. C_q values were normalized to a minimum of two housekeeping reference genes, and changes in expression were calculated using the $2^{-\Delta\Delta CT}$ method (49). Three independent experiments were performed ($n = 3$), and each sample was assayed in duplicate on a CFX Connect Real Time PCR machine (BioRad).

Immunocytochemistry and EdU Labeling. Cultures were fixed with 4% (wt/vol) paraformaldehyde and permeabilized with 0.1% (vol/vol) Triton X-100. Following blocking with 2% (wt/vol) BSA and 5% (vol/vol) donkey serum, cells were incubated with primary antibodies overnight at 4 °C, followed by incubation with complementary Alexa Fluor-conjugated antibodies and counterstaining with DAPI. All antibodies used are listed in *SI Materials and Methods*. To quantify proliferation, differentiating cultures were incubated with 5 μM EdU for 30 min before fixation. EdU detection was then carried out using the Click-iT EdU Alexa Fluor 488 Imaging Kit (Life Technologies). Images were subsequently acquired using an inverted microscope (DMI600b; Leica Microsystems). Manual cell counts were performed on a minimum of 10 randomly placed fields of view per stain, and the mean of three separate differentiations was calculated ($n = 3$).

Embryo sections (6–8 μm) were fixed overnight in 4% paraformaldehyde/PBS, dehydrated, paraffin-embedded, and then processed as described previously (14). For quantification of cells expressing Tubb3, cells of the entire dorsal telencephalon at the medial level were counted; at least two embryos of each genotype were analyzed, with a quantification of three to six sections per embryo.

Cell Cycle Analysis by Flow Cytometry. NPCs were dissociated with EDTA, washed in PBS, and fixed with ice-cold 70% ethanol. After washing with 1% BSA, cell samples were incubated with mouse anti-Nestin (BD Biosciences; 611659, 1 μg/mL) or mouse IgG isotype (Sigma-Aldrich; I5381, 1 μg/mL) antibodies overnight at 4 °C. After incubation with donkey anti-mouse Alexa Fluor 647 secondary antibody (Thermo Fisher Scientific; A-31571, 1:1,000), DNA content was labeled by incubating cells with 1 μg/mL DAPI. Stained cells were analyzed on an Amnis Flowsight (Merck Millipore) under excitation from 405-nm and 642-nm lasers. IgG isotype control samples were used to set gating parameters for Nestin$^+$ NPC and DAPI staining to identify cells at different stages of the cell cycle. Samples from three individual differentiation experiments were analyzed for each time point ($n = 3$).

RNA-seq. RNA was extracted and purified using the PureLink RNA Mini Kit (Thermo Fisher Scientific). The TruSeq Stranded mRNA kit (Illumina) was used to prepare libraries from 1 μg of RNA from three independent differentiations ($n = 3$). The 75-bp paired-end sequencing was performed with the Illumina HiSeq 4000 sequencing system, yielding 30–45 million reads per sample. Reads were mapped to the mouse genome (mm10, GRCm38) using Burrows–Wheeler aligner algorithms (50), and individual gene read counts were calculated using featureCounts (51). DeSeq2 was used to calculate differential gene expression (52). GO functional enrichment for biological processes was performed using DAVID version 6.8 with the *Mus musculus* genome set as background (53). Calculated *P* values were adjusted for multiple testing using Benjamini–Hochberg correction. Raw sequence data files are publicly available from the National Center for Biotechnology Information's Gene Expression Omnibus (accession no. GSE90827).

Luciferase Reporter Assays. Point mutations were introduced into the p*Hes1* (2.5k)-luc firefly luciferase vector using the QuikChange II XL Site-Directed Mutagenesis Kit (Agilent Technologies) and the following mutagenic primers (5′→3′): CAAGGTAAAGAGGATGTGTTCCTCTAATGTCTTCCGGAATT and AATTCCGGAAGACATTAGAGGAACACATCCTCTTTACCTTG for Bs1; and GAAAGTTCCTGTGGGAAAGAAAGTTTGGGAAGTTTCAC and CAAACTTTCTTTCCCACAGGAACTTTCAGCCAATGG for Bs2. Generation of mutagenized plasmids were confirmed by Sanger sequencing.

For luciferase reporter assays, cells were cultured in 24-well plates and cotransfected with 290 ng/well of firefly luciferase [p*Hes1*(2.5k)-luc and its derivatives]. *Renilla* luciferase vector (pGL4.73; 10 ng/well) served as an internal control to normalize for transfection efficiency, and 50 ng of notch intracellular domain (NICD; pCAG-NotchIC-IP) served as a positive control. Cells were harvested at 24 h posttransfection and processed using the Dual-Glo Luciferase Assay System (Promega). Luciferase activity was measured with GloMax 96 Microplate Luminometer (Promega). Triplicate readings were taken for each sample, and all experiments were repeated with three biological replicates ($n = 3$).

ChIP. Approximately 10^7 cells on day 8 of differentiation were used for each immunoprecipitation. Protein and DNA were cross-linked with 1% formaldehyde before cell lysis. The extracted chromatin was subsequently sonicated at high power for 20 cycles of 30 s on/30 s off with a Bioruptor (Diagenode). Immunoprecipitation was performed by incubating chromatin with custom rabbit anti-Dmrta2 or rabbit IgG isotype control antibodies and salmon sperm DNA/Protein A agarose beads (Merck Millipore). Following denaturation of cross-links, Dmrta2-bound DNA fragments were purified using the Wizard SV Gel and PCR Clean-Up System (Promega). Immunoprecipitated DNA was subsequently amplified in qPCR reactions using the primers specified in Table S1. Three immunoprecipitations, each from a separate differentiation experiment, were performed ($n = 3$).

Statistical Analysis. Statistical analyses were performed using IBM SPSS 20 software. Where specified, two-way ANOVA tests were performed, using Dmrta2 genotype status and day of differentiation as independent variables. Simple effects analysis by the post hoc Sidak test was used to correct for separate orthogonal comparisons between groups at each time point and to identify statistical significance. For luciferase assays and siRNA knockdown experiments, one-way ANOVA with Tukey's honest significant difference (HSD) post hoc test were performed. One-tailed and two-tailed Student's *t* tests were used to analyze ChIP-qPCR and *Hes1* transfection rescue experiments, respectively.

ACKNOWLEDGMENTS. We thank Dr. Sally Lowell for the pCAG-NotchIC, Dr. Ryoichiro Kageyama for the Hes1-luciferase vectors, Dr. David Zarkower for the Dmrta2 conditional knockout mice, and Dani Cabezas de la Fuente and Dr. Robert Andrews for invaluable assistance with the bioinformatics analysis. RNA sequencing was performed at the Oxford Genomics Centre. This work is funded by the UK Medical Research Council and Cardiff Neuroscience and Mental Health Research Institute.

1. Caviness VS, Jr, et al. (2003) Cell output, cell cycle duration and neuronal specification: A model of integrated mechanisms of the neocortical proliferative process. *Cereb Cortex* 13:592–598.
2. Miyata T, Kawaguchi D, Kawaguchi A, Gotoh Y (2010) Mechanisms that regulate the number of neurons during mouse neocortical development. *Curr Opin Neurobiol* 20: 22–28.
3. Seo S, Lim JW, Yellajoshyula D, Chang LW, Kroll KL (2007) Neurogenin and NeuroD direct transcriptional targets and their regulatory enhancers. *EMBO J* 26:5093–5108.
4. Gohlke JM, et al. (2008) Characterization of the proneural gene regulatory network during mouse telencephalon development. *BMC Biol* 6:15.
5. Sansom SN, et al. (2009) The level of the transcription factor Pax6 is essential for controlling the balance between neural stem cell self-renewal and neurogenesis. *PLoS Genet* 5:e1000511.
6. Imayoshi I, Kageyama R (2014) bHLH factors in self-renewal, multipotency, and fate choice of neural progenitor cells. *Neuron* 82:9–23.
7. Urquhart JE, et al. (2016) DMRTA2 (DMRT5) is mutated in a novel cortical brain malformation. *Clin Genet* 89:724–727.
8. Bellefroid EJ, et al. (2013) Expanding roles for the evolutionarily conserved Dmrt sex transcriptional regulators during embryogenesis. *Cell Mol Life Sci* 70:3829–3845.
9. Gennet N, et al. (2011) Doublesex and mab-3-related transcription factor 5 promotes midbrain dopaminergic identity in pluripotent stem cells by enforcing a ventral-medial progenitor fate. *Proc Natl Acad Sci USA* 108:9131–9136.
10. Yoshizawa A, et al. (2011) Zebrafish Dmrta2 regulates neurogenesis in the telencephalon. *Genes Cells* 16:1097–1109.
11. Xu S, Xia W, Zohar Y, Gui JF (2013) Zebrafish dmrta2 regulates the expression of cdkn2c in spermatogenesis in the adult testis. *Biol Reprod* 88:14.
12. Saulnier A, et al. (2013) The doublesex homolog Dmrt5 is required for the development of the caudomedial cerebral cortex in mammals. *Cereb Cortex* 23: 2552–2567.
13. Konno D, et al. (2012) The mammalian DM domain transcription factor Dmrta2 is required for early embryonic development of the cerebral cortex. *PLoS One* 7:e46577.

14. De Clercq S, et al. (2016) DMRT5 together with DMRT3 directly controls hippocampus development and neocortical area map formation. Cereb Cortex https://doi.org/10.1093/cercor/bhw384.
15. Caronia-Brown G, Yoshida M, Gulden F, Assimacopoulos S, Grove EA (2014) The cortical hem regulates the size and patterning of neocortex. *Development* 141: 2855–2865.
16. Hirabayashi Y, et al. (2004) The Wnt/β-catenin pathway directs neuronal differentiation of cortical neural precursor cells. *Development* 131:2791–2801.
17. Ying QL, Stavridis M, Griffiths D, Li M, Smith A (2003) Conversion of embryonic stem cells into neuroectodermal precursors in adherent monoculture. *Nat Biotechnol* 21: 183–186.
18. Gaspard N, et al. (2008) An intrinsic mechanism of corticogenesis from embryonic stem cells. *Nature* 455:351–357.
19. Cambray S, et al. (2012) Activin induces cortical interneuron identity and differentiation in embryonic stem cell-derived telencephalic neural precursors. *Nat Commun* 3: 841.
20. Chambers SM, et al. (2009) Highly efficient neural conversion of human ES and iPS cells by dual inhibition of SMAD signaling. *Nat Biotechnol* 27:275–280.
21. Watanabe K, et al. (2005) Directed differentiation of telencephalic precursors from embryonic stem cells. *Nat Neurosci* 8:288–296.
22. Bertacchi M, Pandolfini L, D'Onofrio M, Brandi R, Cremisi F (2015) The double inhibition of endogenously produced BMP and Wnt factors synergistically triggers dorsal telencephalic differentiation of mouse ES cells. *Dev Neurobiol* 75:66–79.
23. Jaeger I, et al. (2011) Temporally controlled modulation of FGF/ERK signaling directs midbrain dopaminergic neural progenitor fate in mouse and human pluripotent stem cells. *Development* 138:4363–4374.
24. Kikkawa T, et al. (2013) Dmrta1 regulates proneural gene expression downstream of Pax6 in the mammalian telencephalon. *Genes Cells* 18:636–649.
25. Barbelanne M, Tsang WY (2014) Molecular and cellular basis of autosomal recessive primary microcephaly. *BioMed Res Int* 2014:547986.
26. Lyden D, et al. (1999) Id1 and Id3 are required for neurogenesis, angiogenesis and vascularization of tumour xenografts. *Nature* 401:670–677.
27. Nakashima K, et al. (2001) BMP2-mediated alteration in the developmental pathway of fetal mouse brain cells from neurogenesis to astrocytogenesis. *Proc Natl Acad Sci USA* 98:5868–5873.
28. Canzoniere D, et al. (2004) Dual control of neurogenesis by PC3 through cell cycle inhibition and induction of Math1. *J Neurosci* 24:3355–3369.
29. Farkas LM, et al. (2008) Insulinoma-associated 1 has a panneurogenic role and promotes the generation and expansion of basal progenitors in the developing mouse neocortex. *Neuron* 60:40–55.
30. Vierbuchen T, et al. (2010) Direct conversion of fibroblasts to functional neurons by defined factors. *Nature* 463:1035–1041.
31. Murphy MW, Zarkower D, Bardwell VJ (2007) Vertebrate DM domain proteins bind similar DNA sequences and can heterodimerize on DNA. *BMC Mol Biol* 8:58.
32. Takebayashi K, et al. (1994) Structure, chromosomal locus, and promoter analysis of the gene encoding the mouse helix-loop-helix factor HES-1: Negative autoregulation through the multiple N box elements. *J Biol Chem* 269:5150–5156.
33. Calegari F, Haubensak W, Haffner C, Huttner WB (2005) Selective lengthening of the cell cycle in the neurogenic subpopulation of neural progenitor cells during mouse brain development. *J Neurosci* 25:6533–6538.
34. Dehay C, Kennedy H (2007) Cell-cycle control and cortical development. *Nat Rev Neurosci* 8:438–450.
35. Tury A, Mairet-Coello G, DiCicco-Bloom E (2011) The cyclin-dependent kinase inhibitor p57Kip2 regulates cell cycle exit, differentiation, and migration of embryonic cerebral cortical precursors. *Cereb Cortex* 21:1840–1856.
36. Castella P, Sawai S, Nakao K, Wagner JA, Caudy M (2000) HES-1 repression of differentiation and proliferation in PC12 cells: role for the helix 3-helix 4 domain in transcription repression. *Mol Cell Biol* 20:6170–6183.
37. Murata K, et al. (2005) Hes1 directly controls cell proliferation through the transcriptional repression of p27Kip1. *Mol Cell Biol* 25:4262–4271.
38. Nguyen L, et al. (2006) p27kip1 independently promotes neuronal differentiation and migration in the cerebral cortex. *Genes Dev* 20:1511–1524.
39. Kawauchi T, Shikanai M, Kosodo Y (2013) Extra-cell cycle regulatory functions of cyclin-dependent kinases (CDK) and CDK inhibitor proteins contribute to brain development and neurological disorders. *Genes Cells* 18:176–194.
40. Heins N, et al. (2001) Emx2 promotes symmetric cell divisions and a multipotential fate in precursors from the cerebral cortex. *Mol Cell Neurosci* 18:485–502.
41. Heins N, et al. (2002) Glial cells generate neurons: The role of the transcription factor Pax6. *Nat Neurosci* 5:308–315.
42. Iacopetti P, et al. (1999) Expression of the antiproliferative gene TIS21 at the onset of neurogenesis identifies single neuroepithelial cells that switch from proliferative to neuron-generating division. *Proc Natl Acad Sci USA* 96:4639–4644.
43. Murphy MW, et al. (2010) Genome-wide analysis of DNA binding and transcriptional regulation by the mammalian Doublesex homolog DMRT1 in the juvenile testis. *Proc Natl Acad Sci USA* 107:13360–13365.
44. Balciuniene J, Bardwell VJ, Zarkower D (2006) Mice mutant in the DM domain gene Dmrt4 are viable and fertile but have polyovular follicles. *Mol Cell Biol* 26:8984–8991.
45. Hirata H, et al. (2002) Oscillatory expression of the bHLH factor Hes1 regulated by a negative feedback loop. *Science* 298:840–843.
46. Bai G, et al. (2007) Id sustains Hes1 expression to inhibit precocious neurogenesis by releasing negative autoregulation of Hes1. *Dev Cell* 13:283–297.
47. Chou SJ, O'Leary DDM (2013) Role for Lhx2 in corticogenesis through regulation of progenitor differentiation. *Mol Cell Neurosci* 56:1–9.
48. Sato T, et al. (2010) FRS2α regulates Erk levels to control a self-renewal target Hes1 and proliferation of FGF-responsive neural stem/progenitor cells. *Stem Cells* 28: 1661–1673.
49. Livak KJ, Schmittgen TD (2001) Analysis of relative gene expression data using real-time quantitative PCR and the 2(-Δ Δ C(T)) method. *Methods* 25:402–408.
50. Li H, Durbin R (2009) Fast and accurate short read alignment with Burrows–Wheeler transform. *Bioinformatics* 25:1754–1760.
51. Liao Y, Smyth GK, Shi W (2014) featureCounts: An efficient general purpose program for assigning sequence reads to genomic features. *Bioinformatics* 30:923–930.
52. Love MI, Huber W, Anders S (2014) Moderated estimation of fold change and dispersion for RNA-seq data with DESeq2. *Genome Biol* 15:550.
53. Huang W, Sherman BT, Lempicki RA (2009) Systematic and integrative analysis of large gene lists using DAVID bioinformatics resources. *Nat Protoc* 4:44–57.